EARTH SURFACE PROCESSES AND LANDFORMS
Earth Surf. Process. Landforms **45**, 2380–2393 (2020)

Published online 18 June 2020 in Wiley Online Library
(wileyonlinelibrary.com) DOI: 10.1002/esp.4886

Estimating the timescale of fluvial response to anthropogenic disturbance using two generations of dams on the South River, Massachusetts, USA

Samantha Dow,[1,2]* Noah P. Snyder,[1] William B. Ouimet,[2] Anna M. Martini,[3] Brian Yellen,[4] Jonathan D. Woodruff,[4] Robert M. Newton,[5] Dorothy J. Merritts[6] and Robert C. Walter[6]
[1] Department of Earth and Environmental Sciences, Boston College, Chestnut Hill, MA USA
[2] Department of Geosciences, University of Connecticut, Storrs, CT USA
[3] Department of Geology, Amherst College, Amherst, MA USA
[4] Department of Geosciences, University of Massachusetts Amherst, Amherst, MA USA
[5] Department of Geosciences, Smith College, Northampton, MA USA
[6] Department of Earth and Environment, Franklin & Marshall College, Lancaster, PA USA

Received 8 February 2020; Revised 23 April 2020; Accepted 24 April 2020

*Correspondence to: Samantha Dow, Department of Geosciences, University of Connecticut, 354 Mansfield Road, Storrs, CT 06269, USA.
E-mail: samantha.dow@uconn.edu

ESPL
Earth Surface Processes and Landforms

ABSTRACT: Centuries-long intensive land-use change in the north-eastern United States provides the opportunity to study the timescale of geomorphic response to anthropogenic disturbances. In this region, forest-clearing and agricultural practices following EuroAmerican settlement led to deposition of legacy sediment along valley bottoms, including behind mill dams. The South River in western Massachusetts experienced two generations of damming, beginning with mill dams up to 6-m high in the eighteenth–nineteenth century, and followed by construction of the Conway Electric Dam (CED), a 17-m-tall hydroelectric dam near the watershed outlet in 1906. We use the mercury (Hg) concentration in upstream deposits along the South River to constrain the magnitude, source, and timing of inputs to the CED impoundment. Based on cesium-137 (^{137}Cs) chronology and results from a sediment mixing model, remobilized legacy sediment comprised 74^{+26}_{-35} % of the sediment load in the South River prior to 1954; thereafter, from 1954 to 1980s, erosion from glacial deposits likely dominated (63 ± 14%), but with legacy sediments still a substantial source (37 ± 14%). We also use the CED reservoir deposits to estimate sediment yield through time, and find it decreased after 1952. These results are consistent with high rates of mobilization of legacy sediment as historic dams breached in the early twentieth century, and suggest rapid initial response to channel incision, followed by a long decay in the second half of the century, that is likely dependent on large flood events to access legacy sediment stored in banks. Identifying sources of sediment in a watershed and quantifying erosion rates can help to guide river restoration practices. Our findings suggest a short fluvial recovery time from the eighteenth–nineteenth century to perturbation during the first half of the twentieth century, with subsequent return to a dominant long-term signal from erosion of glacial deposits, with anthropogenic sediment persisting as a secondary source. © 2020 John Wiley & Sons, Ltd.

KEYWORDS: legacy sediment; dams; mercury; sediment fingerprinting; sediment yield

Introduction

Human alterations to streams, such as dam construction, channel straightening, or riparian deforestation, often result in a myriad of consequences to natural processes, including interruptions to flow and sediment-transport regimes (Poff et al., 2013; Magilligan and Nislow, 2005). These changes can have lasting impacts on channel morphology for decades to centuries, and restoration attempts are often challenging, as pre-disturbance conditions may be unknown (Poff et al., 1997). Dam removal, in particular, is one example of a means to attempt to restore a channel to its pre-disturbance state (Foley et al., 2017). However, the timescale of fluvial response, or resilience, to anthropogenic perturbations is not well constrained, raising questions regarding the return of a system to its pre-disturbance state (e.g. Merritts et al., 2013; Thoms et al., 2018).

Legacy sediments associated with past land uses including forest clearing and dam construction fill valley bottoms in many parts of the world (e.g. James, 2013; Macklin et al., 2014; Stout et al., 2014; Wohl, 2015; Dearman and James, 2019; James, 2019; Johnson et al., 2019). Many legacy sediment studies have been done on streams impacted by widespread historic damming in the Mid-Atlantic region of the eastern United States (e.g. Walter and Merritts, 2008; Merritts et al., 2013; Donovan et al., 2016; Pizzuto et al., 2016). The entire north-eastern United States also has a history of anthropogenic modifications, including deforestation, dam construction, reforestation, and dam removal, and provides the opportunity to study the timescales of geomorphic response to

watershed disturbance. Deforestation, up to 60–80% clearance (Francis and Foster, 2001), and resulting soil erosion led to elevated sediment yield from hillslopes. The concurrent construction of mill dams beginning in the late 1600s in the eastern United States aided in the widespread impoundment of sediment in valley bottoms (Walter and Merritts, 2008; Johnson et al., 2019). Region-wide reforestation (up to 65–90%; Francis and Foster, 2001), dam breaching and removal, and on-going erosion of legacy sediment all influence the geomorphic response over the past ~150 years. Studies quantifying bank erosion of legacy sediment using historical aerial photographs and maps typically span a few decades (e.g. Walter and Merritts, 2008; Donovan et al., 2015), but this interval usually postdates extensive dam breaching. Further, the timescale over which stream channels respond to these disturbances and completely erode legacy deposits is unknown.

However, recent monitoring studies of dam removals measure monthly to yearly timescales of geomorphic changes to the channel (e.g. Doyle et al., 2003; Sawaske and Freyberg, 2012; Foley et al., 2017; Major et al., 2017). A recent compilation of ~20 studies by Major et al. (2017) found that in nearly all cases erosion rates were most rapid in the first year after dam removal. Studying two sand-filled reservoirs in the north-eastern United States, Collins et al. (2017) found that > 50% of impounded sediment was removed within two months of dam removal. These findings are consistent with conceptual models that predict a rapid initial response of channel incision (e.g. Doyle et al., 2002; Pizzuto, 2002). To our knowledge, no dam removal studies address longer timescale processes (10+ years) following breaching, which may allow for removal of the remainder of the deposit, including historic sediment stored in terraces adjacent to the incised channel. Therefore, a knowledge gap exists between short-term dam-removal studies and longer-term legacy sediment erosion studies that typical begin decades after dam breaching. Here, we seek to bridge this gap by applying a suite of methods that allow us to quantify channel and watershed responses to dam removal and land-use change over a century-long timescale.

In the South River watershed of western Massachusetts, USA, large volumes of legacy sediment blanket the valley bottoms (Johnson et al., 2019; Figure 1). Much of this was deposited behind more than 30 eighteenth–nineteenth century mill dams, most of which breached naturally in the past ~150 years. Sediment cores collected from the infilled reservoir behind the Conway Electric Dam (CED), an intact 17-m-tall dam built in 1906, ~1 km upstream from the confluence of the Deerfield River, provide a record of twentieth century erosion from the watershed upstream. This is therefore an ideal location to examine the rate of legacy sediment erosion upstream following historic dam breaches over a timescale that includes the initial, rapid phase from reservoirs and the long tail of erosion of channel banks.

We hypothesize that the most rapid rates of upstream legacy sediment erosion recorded by the CED deposit occurred early in the twentieth century, when or soon after many of the mill dams breached. Second, guided by previous studies suggesting ongoing high rates of legacy sediment erosion (e.g. Walter and Merritts, 2008; Merritts et al., 2013), we propose that legacy sediment sources led to increased fluvial sediment supply throughout the entire twentieth century. These expectations

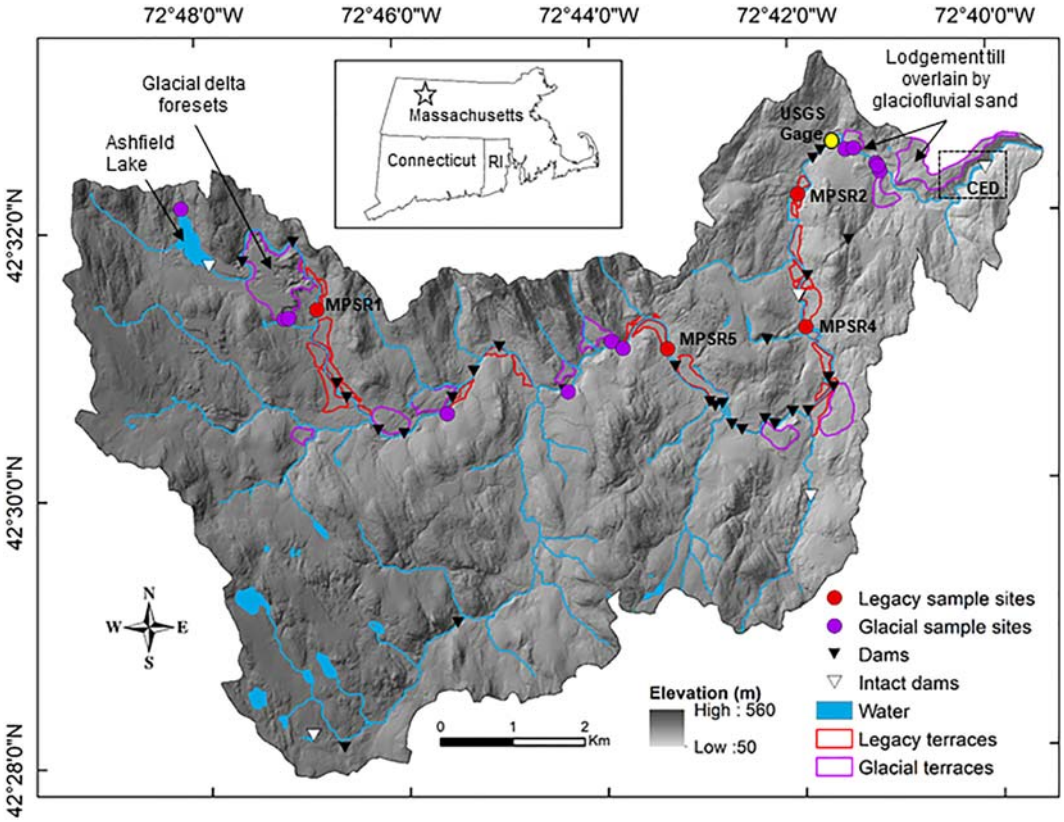

FIGURE 1. Location map of the South River watershed in western Massachusetts (inset), base map is 2 m LiDAR with hillshade overlay. Sampling sites of legacy sediment (red circles) and glacial sediment (purple circles) are shown. Historic dams along the mainstem river (including the Conway Electric Dam [CED]; Figure 4) are denoted by black triangles. Yellow circle represents the location of USGS gage site 01169900. Mapping of legacy sediment deposits along the mainstem river is from Johnson et al. (2019); mapping of glacial-age terraces was completed by field observations and interpretation of LiDAR imagery, largely based on height above the channel, and were focused solely along the mainstem. [Colour figure can be viewed at wileyonlinelibrary.com]

imply that the CED reservoir sediment is derived primarily from erosion and remobilization of formerly impounded mill dam sediment, not mass wasting of glacial deposits that dominate the surface geology of the watershed. We test these hypotheses by reconstructing sediment yields from the CED reservoir sediment, and developing a simple mixing model based on the observation that industrial-age legacy sediment has a higher mercury (Hg) concentration than glacially derived sediment (e.g. till and outwash), distinguishing the two sources. By treating Hg as a tracer along with analysis of historic aerial photographs, we use accumulation behind two generations of dams to estimate the fluvial response time to anthropogenic disturbances.

Study Area

The South River originates in Ashfield Lake, a natural lake enlarged by a 5-m dam, and flows for 25 km through the towns of Ashfield and Conway, to its junction with the Deerfield River (Figure 1). The bedrock geology of the 68 km^2 watershed is characterized by Devonian micaceous schists interbedded with calcareous schists (Emerson, 1898). During Pleistocene deglaciation, the northward-flowing drainage was blocked by ice that formed lakes, and glacial-age sediments along the valley include lacustrine deposits, till, and coarse stratified deposits (Stone and DiGiacomo-Cohen, 2010; MassGIS, 2015). Several 30–40 m thick outcrops exist along the mainstem, which are composed of lodgement till overlain by several meters of glacio-fluvial sand (Figure 1). These outcrops display evidence of mass wasting related to large storm events, such as Tropical Storm Irene in 2011 (Field, 2013). In addition, foreset sediments from a glacial-age delta that fed into a small lake that filled this valley following the last glaciation are exposed in sand quarries in the upper watershed. At present, most sediment entrainment in steep, post-glacial watersheds in New England is from fluvial erosion of glacial sediments, and not from rill erosion or agricultural sources (Yellen et al., 2014; Dethier et al., 2016), where glacial sediment is accessed through gullying and riverbank mass wasting events that are reactivated during high flow events. Thus, for this study, we assumed minimal topsoil erosion (Tomer and Locke, 2011; Fox et al., 2016), and focused on two primary sediment sources: (1) near channel mass wasting of glacial overburden; (2) exposed banks of legacy sediment. These were noted by Field (2013) to be the main contributors to the sediment load. We sampled both types extensively along the mainstem of the South River (Figure 1).

Historic land-use activity in the watershed was primarily logging and pasturing, and up to ~80% of land was cleared by the early 1800s (Francis and Foster, 2001; Foster and Motzkin, 2009). The first generation of dams constructed for milling began in Ashfield in 1744, and 32 mills with dams up to 6-m tall operated throughout the watershed until the early twentieth century (Howes, 1910; Field, 2013; Johnson et al., 2019). Manufacturing activities subsequently decreased, and most of the remaining mills were abandoned between 1904 and 1916 (Barten and Kantor, 2013; Field, 2013). Although minimal documentation exists on when the mill dams were removed or breached, many dams were damaged and repaired after a flood in 1869 (Barten and Kantor, 2013). The Tucker and Cook Dam, downstream of sample site MPSR5 (Figures 1, 2), was dismantled following the 1936 freshet, and extensive damage occurred along the river due to flooding from a Category 3 hurricane in 1938, likely breaching most of the remaining dams (Jahns, 1947; Barten and Kantor, 2013). Analysis of 1940 aerial photographs shows evidence of few intact dams remaining on the South River and its tributaries at that time.

While all dams raise base level and provide opportunities for impoundment of sediment in upstream channels and floodplains, smaller, channel spanning run-of-the-river dams and inset dams (versus those that span the entire alluvial valley) can store less (e.g. Merritts et al., 2013; Pearson and Pizzuto, 2015). In the South River watershed, several of the dams associated with milling show clear evidence of sediment impoundment. The Tucker and Cook Dam (site MPSR5) was a 6-m tall granite block dam that created a large reservoir in order to store water for downstream mills (Figure 2; Field, 2013; Johnson et al., 2019). At present, up to 3.5-m-high banks of impounded sediment remain following its partial removal in 1936. Site MPSR1 similarly shows evidence of a 90-m-wide, valley-spanning former mill dam that impounded sediment up to 2-m thick (Figure 3; Field, 2013). Johnson et al. (2019)

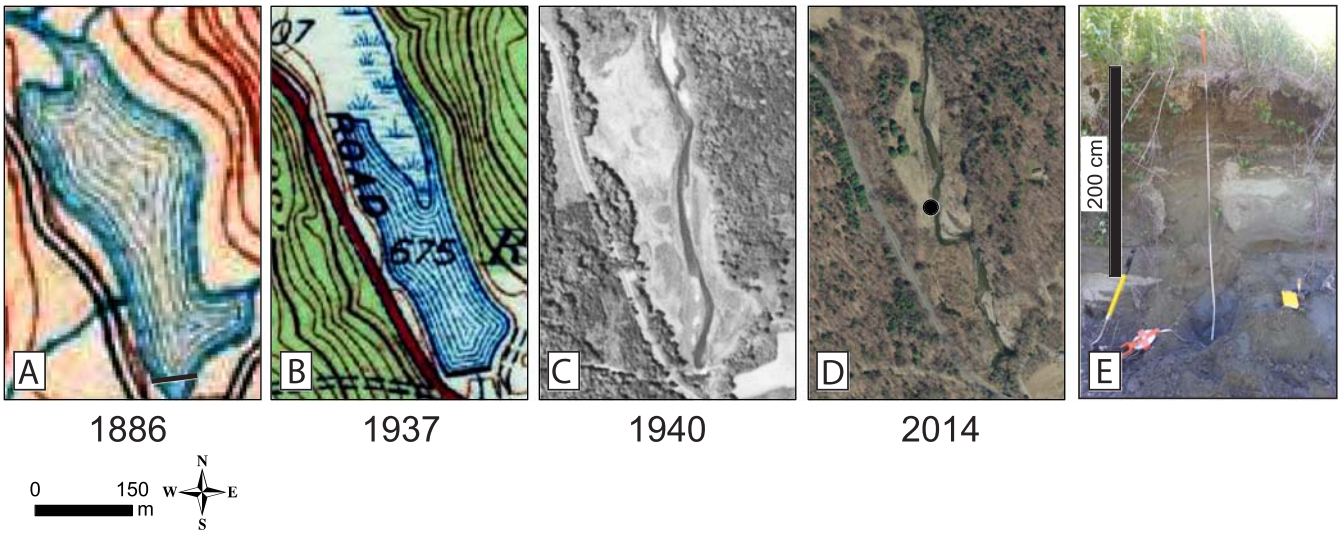

FIGURE 2. Topographic (A, B) and aerial imagery (C, D) of site MPSR5, at the former location of the 6-m-tall Tucker and Cook Dam, built in 1837, which created a large reservoir. The dam was partially removed in 1936, following a flood (Barten and Kantor, 2013; Field, 2013). The 1940 aerial imagery (C) shows the channel incised through the former impounded sediment. Black line on the 1886 map (A) represents the dam location; black dot on 2014 map (D) shows sampling location. (A)–(D) All shown at the same scale. (E) Field photograph of the sampling location. [Colour figure can be viewed at wileyonlinelibrary.com]

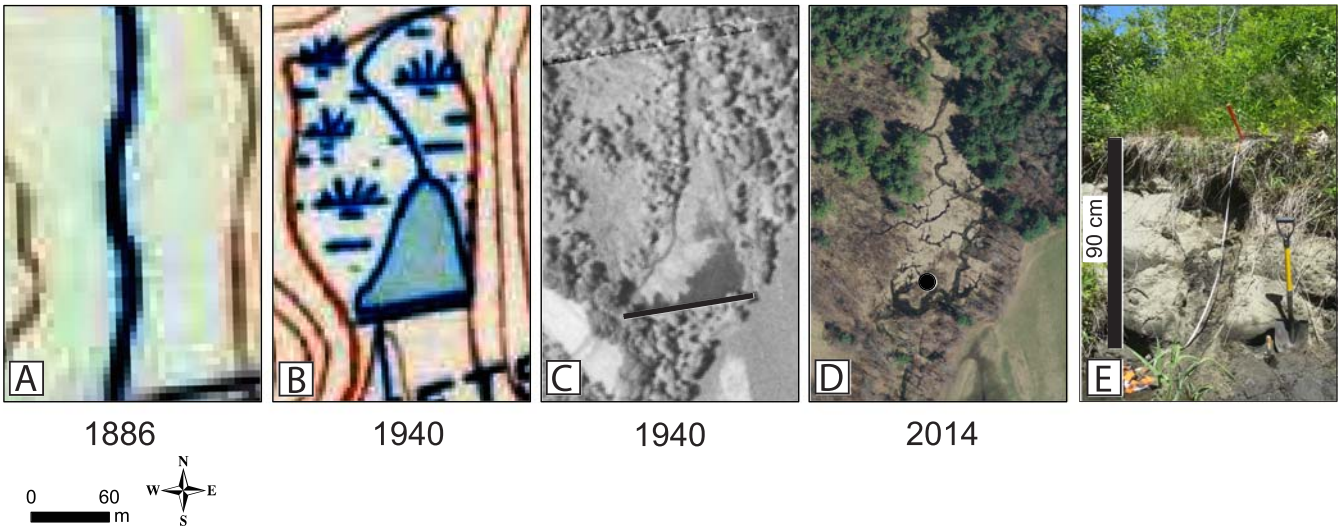

FIGURE 3. Topographic (A, B) and aerial imagery (C, D) at site MPSR1 showing the presence of a twentieth century mill dam and reservoir. No reservoir is shown on the 1886 map, however, a dam may have existed at this site and was washed out in an 1878 flood (Field, 2013). The dam breached sometime between 1940 and 1970, based on interpretation of aerial imagery. Black dot on the 2014 map (D) shows sampling location. (A)–(D) All shown at the same scale. (E) Field photograph of the sampling location. [Colour figure can be viewed at wileyonlinelibrary.com]

estimated that the watershed contains $1.9\times10^6 \pm 7.9\times10^5$ m^3 of legacy sediment in the valley bottoms, which includes millpond and non-millpond deposits associated with the period since land clearing by EuroAmerican settlers (Figure 1).

The second generation of dam construction in the watershed occurred in 1906, with the completion of the CED for hydroelectricity to power a trolley car. The CED is a 17-m tall concrete structure located 1 km upstream from the Deerfield River (Figures 1, 4). The reservoir impounded by the dam acts as a trap for sediment eroded from the 99% of the South River watershed that is upstream of the dam. It is one of three dams currently remaining on the mainstem river (Figure 1).

Methods

Sediment sampling and processing

Four 7.6 cm diameter sediment cores (VC1 333 cm; VC2 290 cm; VC3 473 cm; VC4 160 cm) were collected in a linear transect in the floodplain within the impoundment adjacent to the South River channel directly upstream of the CED using a vibracore apparatus in July 2013 (Figure 4). An additional vibracore (VC5) measuring 500 cm was collected in the reservoir deposit 450 m upstream of these cores in May 2017 (Figures 1, 4). Cores were sampled at every 10-cm in 1 cm

FIGURE 4. (A) Photograph of researchers standing on impounded sediment in the channel just upstream of the Conway Electric Dam (CED), which is on the left side of image. (B) A 2014 aerial orthophotograph of the CED impoundment (30 cm resolution; from MassGIS) and vibracore locations at this site. [Colour figure can be viewed at wileyonlinelibrary.com]

increments and any layer with a notable change in stratigraphy within the interval was also sampled.

We selected sites for sampling legacy (anthropogenic sediment accumulated behind mill dams) and glacial-age sediment based on interpretations of features in LiDAR (light detection and ranging) imagery, previously mapped legacy sediment terraces by Johnson et al. (2019), previously published geologic mapping by Stone and DiGiacomo-Cohen (2010), and field observations. Samples were collected in June 2016 from 11 actively eroding glacial-age outcrops (n = 11) and in vertical profiles at four eroding legacy exposures upstream of breached mill dams (n = 57) along the mainstem of the South River (Figure 1). Locations of the sites were obtained using a handheld Trimble Juno SB unit and a real-time kinematic (RTK) Leica Viva GNSS GS14 Rover.

Glacial, legacy, and CED (VC3 and VC5) sediment samples were oven dried at 60 °C for geochemical and grainsize analyses. Samples were analyzed using loss on ignition (LOI) to determine organic content for dried samples using standard procedures (Dean, 1974). Of the four cores collected in 2013 (VC1, VC2, VC3, VC4), geochemical analyses were only completed on VC3, as it was the longest of the four recovered, and all are presumably similar because of their close proximity and similar grain size and organic concentrations. We measured bulk density every 10 cm for both VC3 and VC5 during the LOI process. The volumes of water, inorganic, and organic material were determined during drying, and combined to calculate the sample total volume, assuming a density of 2.65 g/cm^3 for clastic sediment, and 1.2 g/cm^3 for organics. Wet bulk density was calculated by dividing the wet mass by the total sample volume. Dry inorganic bulk density was calculated by multiplying the wet bulk density value by the mass of clastic sediment (post-LOI) and dividing by the mass of the entire wet sample.

Post-LOI samples were dispersed using 0.2% sodium metaphosphate, then wet-sieved at 63 μm to obtain the weight percent for the < 63 μm fraction. Sediment in the > 63 μm fraction was analyzed using a Horiba CAMSIZER Digital Image Processing Particle Size Analyzer in order to obtain weight percentages in 100 size classes from 63 μm to 1 cm. Cumulative grain-size distributions and D_{10}, D_{50}, and D_{90} values (the grain size for the percentage of the sample finer than this diameter) for the entire distribution (< 63 μm fraction added to the > 63 μm fraction) were calculated using the program Gradistat Version 8.0 (Blott and Pye, 2001).

Dried sub-samples were homogenized for Hg and cesium-137 (^{137}Cs) analyses by powdering with a mortar and pestle. Direct combustion analyses for Hg were conducted on 0.05–0.1 g of sediment using a Teledyne Leeman Labs Hydra-C mercury analyzer with cold vapor atomic absorption. All Hg concentrations were normalized for organic content by diving the LOI value for that sample because Hg has a high affinity for organics. Generally, samples with $D_{50} > 200$ μm were not analyzed for Hg, as Hg does not concentrate on coarser sediment due to low surface area (Horowitz and Elrick, 1987). Therefore, measurements were focused on fine-grained or organic-rich sediment. Hg analyses for VC3 were completed from 200 to 473 cm, as the sediment in the upper portion of the core was medium sand or coarser.

We used the presence of ^{137}Cs associated with nuclear weapons testing to constrain the chronology of VC3 and VC5 (Pennington et al., 1973). Sample layers with D_{50} < 200 um (four from VC3, four from VC5, each 25–30 g) were collected and homogenized, and ^{137}Cs concentrations were measured using gamma spectrometry on a Canberra GL2020R Low Energy Germanium Detector. We also measured lead-210 (^{210}Pb), but down-core changes in the activity of this short-lived radioisotope are complicated in depositional environments where rates and characteristics of sedimentation may vary (Kirchner, 2011), and therefore was not used in our geochronological analysis. The presence or absence of ^{137}Cs was used to determine if sediment in the CED was deposited after or before 1954, respectively. Our coarse sampling interval did not permit more detailed geochronologic interpretations, such as the location of the ^{137}Cs peak (Pennington et al., 1973).

Reservoir change analysis

We used georeferenced aerial photographs from 1940, 1952, 1972, and 1981 to measure the progradation of the delta into the CED reservoir (Figure 5). The longitudinal stream profile was obtained from a LiDAR 2-m horizontal resolution digital elevation model (DEM, 2012 data; OCM, 2020). We then estimated the 1906 pre-dam profile by manually projecting a straight line from the upstream end of the CED impoundment to the bottom of the dam (Figure 6). The difference between the 2012 and 1906 interpreted pre-dam profile, in combination with ^{137}Cs interpretation from VC3 and VC5 (Figures 7, 8), was used to estimate the depth of the impoundment deposit at each delta front position. The total volume of sediment stored behind the dam was calculated using the area of the sediment mapped, along with the average depth of the sediment, assuming that the valley bottom is V-shaped (McCusker and Daniels, 2008). Similarly, the sediment volume for each interval between aerial photographs contains both the sediment area of the prograding delta and the amount of sediment located in front of the delta, forming the foreset and bottomset, and also assumes a V-shaped valley bottom. Sediment yields through time were calculated following the methods of McCusker and Daniels (2008), and were converted from m^3 to t/yr/km^2 using our measured average inorganic-fractioned dry bulk sediment density, and a watershed area of 68 km^2.

Eroded legacy sediment analysis

To provide a rough comparison with sediment stored in the CED reservoir, we estimated the maximum volume of legacy sediment removed from the channel from behind former mill dams using a LiDAR analysis along reaches of the channel where the adjacent banks are composed of legacy sediment (Figure 1; Johnson et al., 2019). Width across the channel was measured at 80 m intervals using aerial photographs (Galster *et al.*, 2008), and topographic profiles generated from the LiDAR DEM across the channel at these width locations were used to determine a bank height corresponding to each width measurement. Average width and heights along the length of the channel for each reach containing legacy sediment were used to calculate the volume of eroded material in m^3. We emphasize that this is a maximum estimate because (1) not all of the mapped legacy sediment was deposited in former mill ponds, and (2) more importantly, channels would have existed within mill ponds as they filled with sediment, even when the dams were in place.

Sediment mixing model

Sediment fingerprinting, or sediment provenance, is a method that has been used in fluvial environments over the past several decades in order to identify sources at the watershed scale,

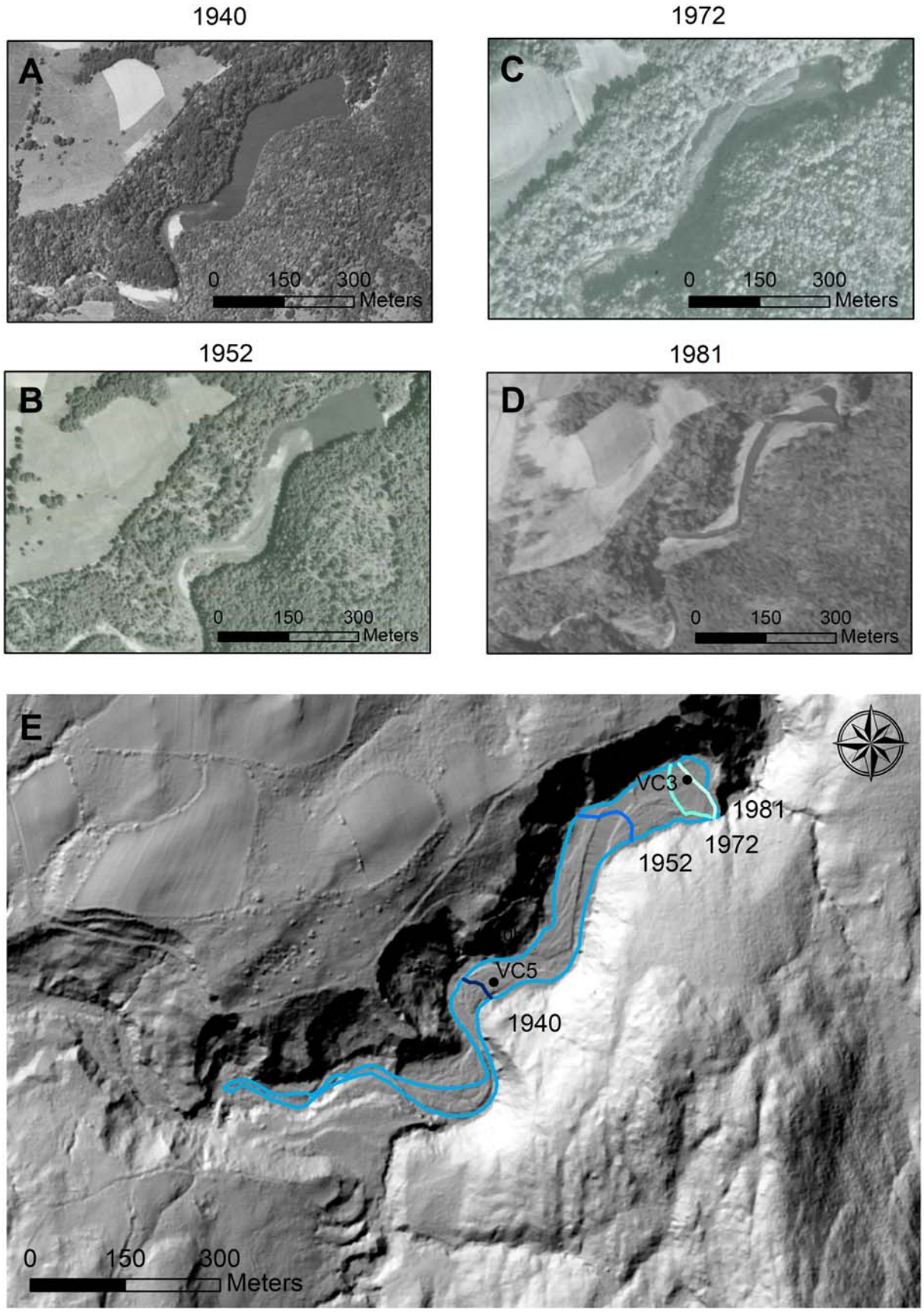

FIGURE 5. Unorthorectified aerial photographs showing Conway Electric Reservoir in (A) 1940, (B) 1952, (C) 1972, and (D) 1981. (E) Map displaying the original extent of the reservoir based on historical documentation stating it reached 1 km upstream of the dam (Pease, 1917) in 1906 (blue polygon), and the progradation of the sediment delta front for the years 1940, 1952, 1972, and 1981. Base map is 2 m LiDAR hillshade. Black dots indicate coring locations; grainsize and geochemical analyses primarily focused on VC3 and VC5. [Colour figure can be viewed at wileyonlinelibrary.com]

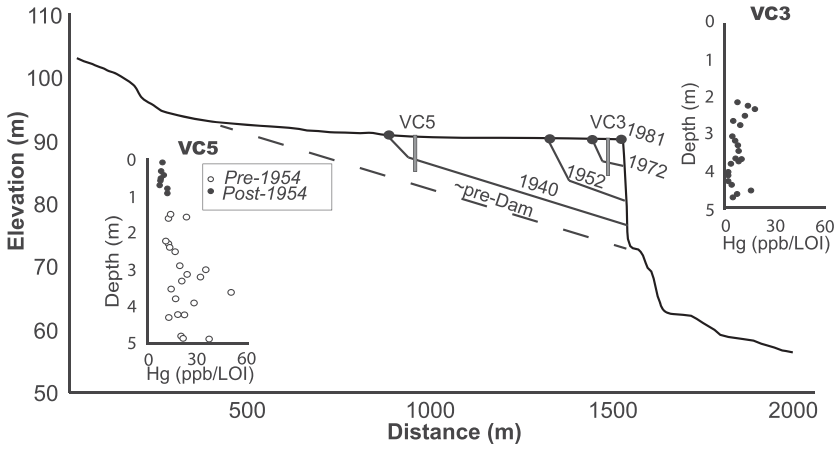

FIGURE 6. Longitudinal transect of the Conway Electric Dam reservoir showing locations and Hg/LOI profiles for vibracores VC3 and VC5 (vertical gray lines). The transect is a smoothed profile generated from LiDAR (2012, 2 m resolution). Dashed line is interpreted pre-dam channel bottom. Thin black lines represent the interpreted delta location determined from aerial photographs (Figure 5). Dates on the cores were determined using the presence or absence of ^{137}Cs. The top half of VC3 was not sampled for Hg because material was primarily sand. The ^{137}Cs detected near the surface of VC5 may be due to overbank floodplain deposition after the reservoir filled at this location.

primarily by analyzing samples of sediment in suspension, but also using samples from river beds, reservoirs, and/or floodplains (Haddadchi *et al.*, 2013). Physical characteristics (color, grain size), bulk geochemistry, mineralogy, mineral magnetic properties, radionuclides, and isotopes (Walling, 2005; Banks et al., 2010; Mukundan et al., 2012; Koiter et al., 2013; Laceby et al., 2017) have all been used in order to differentiate among sediment sources. Many studies have used mixing models as quantitative assessments to evaluate statistically relative contributions of different source areas (Collins et al., 1998; Banks et al., 2010; Gellis and Walling, 2011; Belmont et al., 2014).

We used a two-end-member mixing model (modified from Palazón et al., 2015) to calculate relative contributions of legacy (x_l) and glacial sources (x_g). This was based on average Hg/LOI concentrations as a tracer in the two sources (Hg_g, Hg_l) and the sink (Hg_{CED}). The fractional relationship for each source is expressed by:

$$x_g + x_l = 1. \tag{1}$$

The unknown contributions are solved by:

$$Hg_g * x_g + Hg_l * x_l = Hg_{CED}. \tag{2}$$

Uncertainty in the mixing model was propagated through Monte Carlo methods (Small et al., 2002), using the average and standard deviation Hg/LOI concentrations of the log normal distributions to generate 10000 random possible end-member concentrations. The log Hg/LOI values were returned to normal concentrations in ppb before being incorporated into the mixing model.

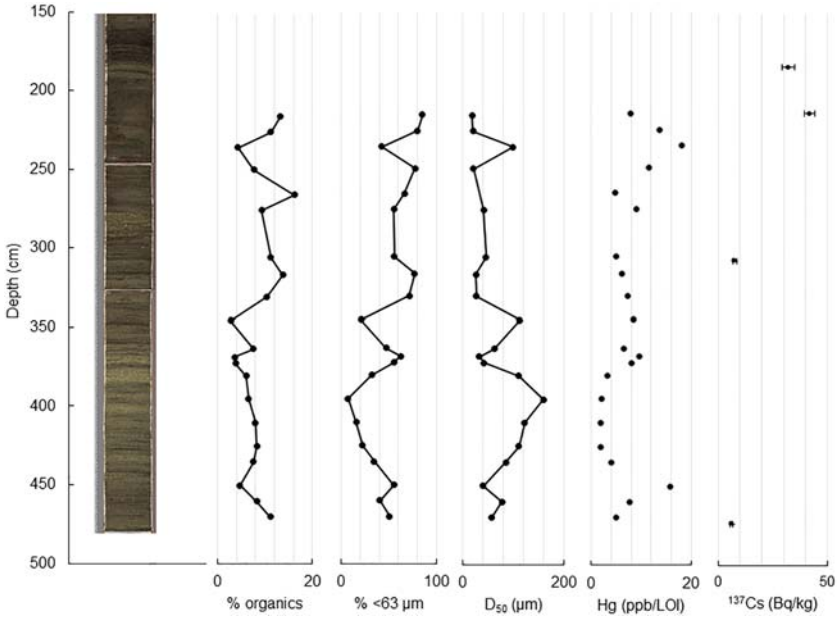

FIGURE 7. Core photograph, percent organics (LOI), percent fines (< 63 µm), median grain size (D_{50}), concentrations of Hg/LOI, and ^{137}Cs measured in the bottom portion of core VC3 at the Conway Electric Dam. The top portion of the core was not sampled for geochemical analyses because material was primarily sand. ^{137}Cs was detected at the bottom of the core, indicating a sediment age younger than 1954. [Colour figure can be viewed at wileyonlinelibrary.com]

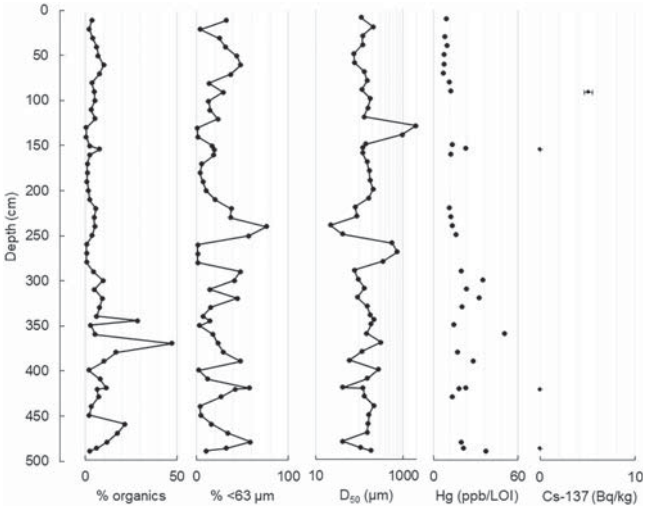

FIGURE 8. Percent organics (LOI), percent fines (< 63 µm), median grain size (D_{50}), and concentrations of Hg/LOI detected in core VC5 at the Conway Electric Dam. ^{137}Cs was detected at a depth of 90 cm, but not in three samples from lower in the core.

Results

Based on dam height and stream gradient, we interpret the backwater of the early CED impoundment (1906) to extend about 1.4 km upstream from the dam (Figures 4–6). Aerial photograph analysis reveals that the subaerially exposed part of the delta that formed in the reservoir had prograded to the dam by 1981.

We estimate that the total volume of sediment trapped and stored in the reservoir is ~244 000 m^3, based on assuming a V-shaped valley bottom (McCusker and Daniels, 2008). For comparison, we estimate that from the time individual dams breached up to modern day, the maximum volume of legacy sediment eroded from sections of the channel upstream of the CED is ~215 000 m^3. The average D_{50} for the reservoir, based on VC3 and VC5, is 241 µm (D_{50} range is 22–3180 µm; n = 123). The average sediment yield based on the CED volume from 1906 to 1981 is 70 ± 14 t/yr/km^2, based on a measured dry sediment bulk density of 1000 ± 200 kg/m^3. Sediment yields during each of the aerial photograph intervals generally decreases from 72 ± 14 t/yr/km^2 between 1906 and 1940 to 5 ± 1 t/yr/km^2 from 1972 to 1981, with the notable exception of 1940 to 1952, when yields doubled (Figure 9; Table 1). These rate calculations assume that the volume of sediment deposited on floodplains and the channel within and upstream of the CED reservoir since 1981 is minimal. However, trapping of bedload by the dam is an ongoing process, as evidenced by the absence of coarse gravel immediately upstream of the CED. Instead, coarse sediment is being deposited near the upstream end of the reservoir deposit where the slope of the stream decreases (Figures 4A, 6).

Results from ^{137}Cs measurements in VC3 and VC5 are consistent with aerial photograph interpretations. Thus, ^{137}Cs was detected at a depth of 473 cm, near the bottom of core VC3 (Figure 7), indicating that all of the cored sediment above this depth was deposited after 1954 (Pennington et al., 1973). In VC5, ^{137}Cs was detected at 90 cm, indicating that the top 90 cm of sediment is younger than 1954, and was likely deposited as a result of overbank floodplain sedimentation after this section of the reservoir filled (Figures 4, 6, 8). Samples between 90 and 154 cm were sandy and too coarse to analyze for ^{137}Cs. However, two samples from fine-grained layers below 154 cm were analyzed, and no ^{137}Cs was detected, indicating sediment deposited prior to 1954.

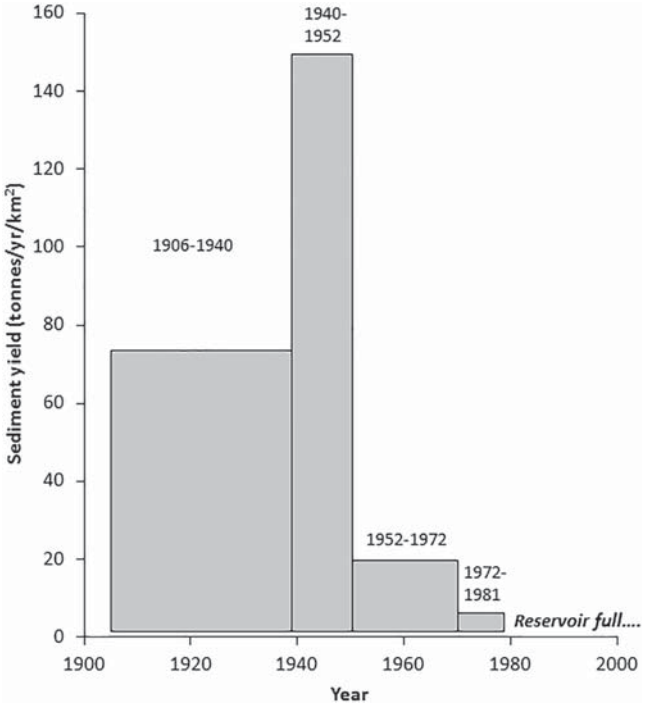

FIGURE 9. Sediment yield estimates calculated from sediment stored behind the Conway Electric Dam. Yield estimates for each of the time intervals correspond to delta front locations mapped in Figure 5(E).

Measured Hg/LOI concentrations in glacial samples (1–4 ppb/LOI; average 2.06 ppb/LOI; n = 11) are lower than in legacy sediment (3–380 ppb/LOI; average 13.36 ppb/LOI; n = 57; Figure 10). While only 11 glacial samples were collected throughout the watershed, we assume that due to their low Hg concentration and low variability, additional samples would not significantly change these results, as discussed further later. Mann–Whitney U tests indicate a statistical significance at the 95% confidence level between the means of the two deposit types ($p = 1.49\times10^{-6}$). Profiles from three of the four legacy sites (MPSR1, MPSR4, MPSR5) have concentrations ~10–20 ppb/LOI (Figures 1, 11). The farthest downstream site (MPSR2) has some layers with higher concentrations, with a peak of up to 380 ppb/LOI occurring at ~100 cm depth. Concentrations in the CED range between 2 and 50 ppb/LOI, and are statistically higher in VC5 (7–50 ppb/LOI) than VC3 (2–18 ppb/LOI; two sample t-test, p = 0.0014; Figure 6). Hg concentration does not appear to be strongly influenced by either organics or grain size (Figure 12).

The mixing model analysis was completed using Hg/LOI concentrations from both VC3 and VC5 to calculate source contributions to the CED reservoir from dam construction in 1906 to infilling by 1981. From this analysis, 32 ± 10% of the sediment is derived from glacial sources and 68 ± 10% from legacy sources upstream. We used the ^{137}Cs geochronology to analyze source contributions for the first and second halves of the twentieth century (Figure 6). This analysis suggests that 26^{+35}_{-26} % is from glacial and 74^{+26}_{-35} % is from legacy deposits from 1906 to 1954. After 1954, 63 ± 14% is from glacial and 37 ± 14% is from legacy deposits.

Discussion

Results from the calculated sediment yield and mixing model allow us to evaluate the role that mill dam breaching had on twentieth century legacy sediment sources and erosion. In addition, they allow for the evaluation of the hypothesis that

Table 1. Calculations of sediment area, average depth, area covered by bottom set deposits in front of the prograding delta, average bottomset depth, volume, and sediment yield for the different intervals between interpreted positions of the delta front (Figure 6)

Time	Sediment area (m^2)	Sediment average depth (m)	Bottomset area (m^2)	Bottomset average depth (m)	Volume (m^3)	Infilling rate (m^3/yr)	Sediment yield (t/yr/km^2)
Photograph Intervals							
1906–1940	20519	4.6	39947	6	166626	4901	72 ± 15
1940a–1952	26168	6.2	13779	6	122066	10172	150 ± 30
1952–1972	10176	4.3	3604	3	27029	1351	20 ± 4
1972–1981	3604	1.8	n/a	n/a	3153	350	5 ± 1
Average							
1906–1981	60467	8.1	n/a	n/a	243983	3253	70 ± 14

increased erosion from anthropogenic legacy deposits remains the primary sediment source, as opposed to mass wasting of glacial deposits, through the twentieth century.

Mixing model findings and limitations

Glacial sediment sources in the South River watershed provide a pre-industrial geochemical baseline for Hg/LOI (1–4 ppb/LOI) to compare with the signal of sediment mobilized during the period since EuroAmerican settlement of the watershed (3–380 ppb/LOI; Figure 10A). Buried glacial sediment has not been exposed to the fallout of high concentrations of trace metals associated with industrialization. Higher concentrations of Hg in legacy sediment (~10–29 ppb/LOI; Figure 11) are attributable to an increase in global atmospheric concentrations produced from coal burning and other industrial activity, which was likely adsorbed to hillslope soils and subsequently eroded during nineteenth century deforestation (Kamman and Engstrom, 2002; Perry et al., 2005). Hg/LOI concentrations up to 380 ppb/LOI at MPSR2 that are not measured at the other legacy sediment locations may be related to local point-source pollution from an upstream (~3 km) hatting shop during the early nineteenth century, as mercury nitrate was used in the processing of fur (Pease, 1917; Varekamp, 2006). MPSR4 also is located downstream of the hatting site, however it does not show high Hg concentrations. While records of dam construction and breaching from this time period are sparse, it is possible that this discrepancy may be related to the timing of construction and infilling of mill dam reservoirs in relation to the timing of the hatting activity.

The Hg/LOI concentrations measured behind the CED require a mix of high-Hg legacy sediment, and low-Hg glacial sediment (Figure 10A). The mixing model using data from cores VC3 and VC5 demonstrates that contributions from legacy sediment sources are higher (68 ± 10%) than glacial sources

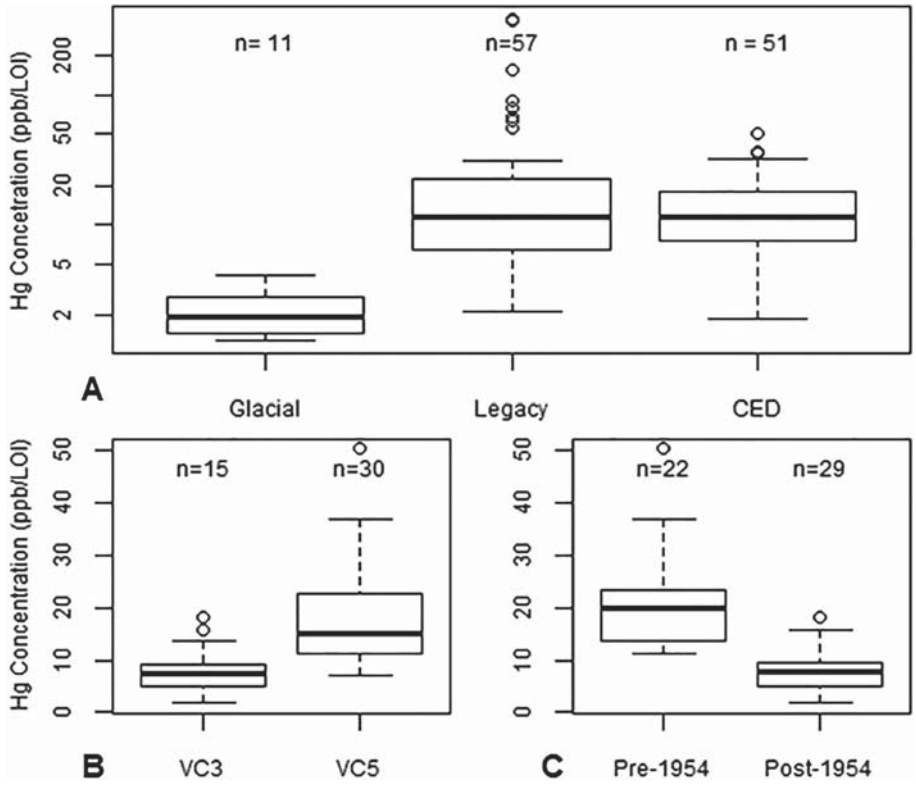

FIGURE 10. Boxplots of mercury concentrations (ppb/LOI) for samples collected from (A) glacial deposits (sediment source), legacy sediment bank exposures (sediment source), and at the Conway Electric Dam (CED) (sediment sink), (B) VC3 and VC5 from the CED, and (C) pre- and post-1954 from VC3 and VC5 at the CED. Concentrations are the lowest in glacial sediment and highest in legacy sediment, and are higher in older sediment deposited behind the CED. Mean and one standard deviation for glacial sediment is 2.06 ppb/LOI (1.37–3.08 ppb/LOI), 13.36 (4.19–42.60) for legacy, and 10.89 (5.26–22.58) for CED. Mean and one standard deviation for VC3 and VC5 are 6.30 ppb/LOI (3.31–11.98) and 15.99 ppb/LOI (9.60–26.63), respectively. Mean and one standard deviation for pre-1954 and post-1954 are 11.32 ppb/LOI (5.17–24.82) and 8.84 ppb/LOI (7.26–10.77), respectively

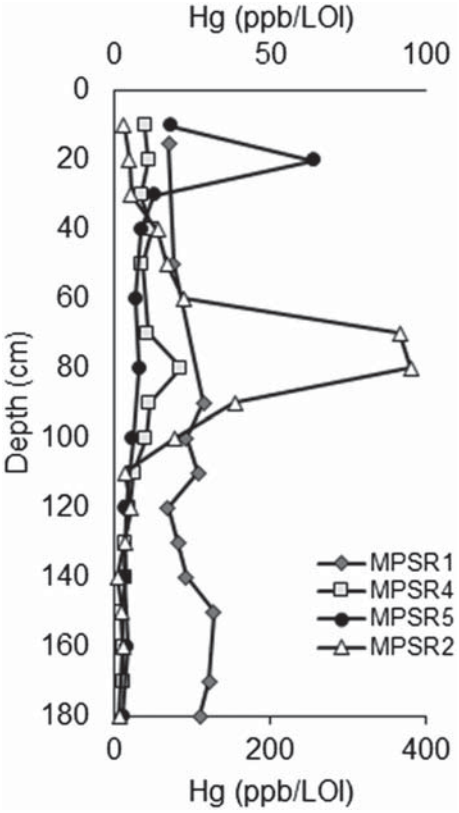

FIGURE 11. Depth profiles of Hg concentration (ppb/LOI) at legacy sediment sites MPSR1, MPSR2, MPSR4, and MPSR5. Hg for MPSR2 (triangles) is displayed on the bottom *x*-axis, concentrations for the other three profiles are displayed on the top *x*-axis.

(Table 2). We conducted a sensitivity analysis to evaluate contributions for the entire deposit excluding the two highest-Hg/LOI outliers from MPSR2 (367 and 380 ppb/LOI; Figure 11). In this calculation, glacial sources contributed 15 ± 36% and legacy deposits contributed 85 ± 36%, suggesting that the dominance of legacy sediment in the CED deposit is likely robust. In addition, Hg concentrations in the CED are overall very similar to legacy sediment (Figure 10A), suggesting legacy sediment is the dominant component. The stored volume of 244 000 m^3 suggests that the reservoir had sufficient accommodation space to store all of the maximum 215 000 m^3 of legacy sediment estimated to have been eroded from upstream mill dam impoundments. This is ~10% of the $1.9\times10^6 \pm 8.0\times10^5$ m^3 of legacy sediment still stored in the watershed (Johnson et al., 2019).

Contributions estimated through the mixing model are subject to assumptions inherent in the approach. Sediment transport dynamics are complex. The model assumes that all sediment particle sizes transported from each source are equally mobile. The glacial till matrix, however, is composed primarily of silt and clay, which can move farther than coarser sediment in suspension. Legacy sediment is coarser, composed of silt and fine sand (the D_{50} at the four sites ranges from 101 to 185 μm; Table 3), which could result in shorter distances traveled and preferential trapping behind the CED. Storage of legacy sediment in locations such as channel bars could reduce loads to the CED and result in an underrepresentation of the legacy contributions.

Our mixing model includes only two different watershed sources and one tracer (Equations (1) and (2)). This simple approach is based on the observation that the most obvious sources of sediment to the modern channel are banks of legacy sediment and mass wasting of glacial deposits. The model does not take into account additional sources, such as gully or rill erosion of hillslope soil. Such features are developed in glacial-age deposits, so Hg concentrations are likely lower than those in legacy sediment, even without the additional Hg that legacy sediment would have received from industrial contamination. Brena et al. (2014) found that soil O horizons in modern deciduous forests in western Massachusetts display a range of Hg values, concentrated near the surface. That suggests that shallow erosion of forest soils could be an important source of Hg, and incorporating additional source types into the model might result in more representative contribution estimates. However, erosion from gullies would access deeper sediment, likely containing lower Hg levels (McCusker Hill and Ouimet, 2015).

Changing sediment sources and yields though the twentieth century

The CED cores contain significantly less Hg/LOI concentrations in layers deposited prior to 1954, compared with those deposited afterward (Figures 6, 10B,C). This observation, along with the sediment yield calculations (Figure 9; Table 3), is consistent with our first hypothesis of greater erosion from upstream legacy deposits early in the CED history.

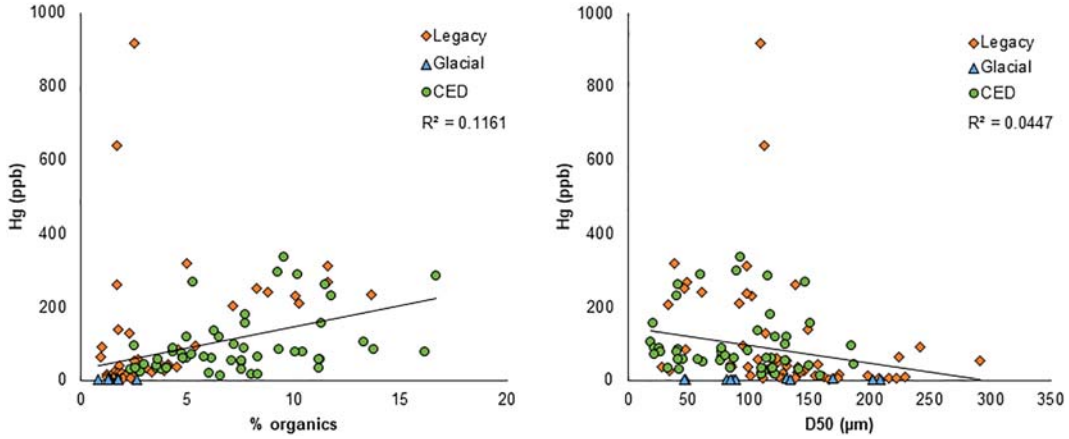

FIGURE 12. (A) Scatter plot showing correlation between organic content (% LOI) and Hg (bulk concentration), and (B) between grain size (D_{50}) and Hg. No significant correlation is observed between Hg concentrations and either grain size or organics. [Colour figure can be viewed at wileyonlinelibrary.com]

Table 2. Grainsizes for the four legacy sediment sites as average D_{50} (μm)

Sample location	Average D_{50} (μm)	D_{50} 1σ range (μm)	Number of samples
MPSR1	142	52–386	18
MPSR2	185	79–430	19
MPSR4	144	110–189	17
MPSR5	101	47–222	14

Sediment yield estimates are up to an order of magnitude higher in the first half of the twentieth century than the second half, when yields decreased to 5–20t/km^2/yr. Annual suspended sediment yields of 8 to 30t/km^2/yr have been measured in the 1980s to the 1990s in southern New England rivers (Kulp, 1983; Kulp, 1991; Bent, 2000). However, we note two limitations of the yield calculations. First, the trapping efficiency of a reservoir decreases through time, and less suspended load may be trapped as storage capacity decreases (Brune, 1953; Verstraeten and Poesen, 2000). By 1981, in the CED reservoir, the delta front had prograded ~100m to the dam (Figure 5). Since then, the opportunity to trap suspended load in the CED reservoir is likely limited to overbank deposition on the newly formed floodplain, and for some decades prior, the reduced reservoir volume likely decreased the efficiency of suspended sediment trapping. Hg data may be influenced by decreasing trap efficiency, however, it is unlikely that the Hg concentrations are influenced by grain size (or organic content) (Figure 12). Further, the average D_{50} of the samples deposited post-1954 (78μm) is statistically finer than pre-1954 (140μm; two sample *t*-test, $p = 0.03$), suggesting either a minimal influence of grainsize on Hg, as Hg is more likely to adsorb to finer sediment, or that this sediment is from low-Hg glacial till deposits. Second, nine of the 10 largest floods at the closest long-term discharge gage (USGS 01168500, Deerfield River at Charlemont, MA), including the 1936 and 1938 floods (Jahns, 1947) that breached several dams on the South River, occurred prior to 1952 (Figure 13). We used this gage as a representation of high flow events for the area because of its long record. However, flow on the Deerfield River has been regulated since 1924, and this gage is located ~25km upstream of the South River confluence, both of which limit its relevance to our study. The gage on the South River has only been operational since 1966 (Figure 13).

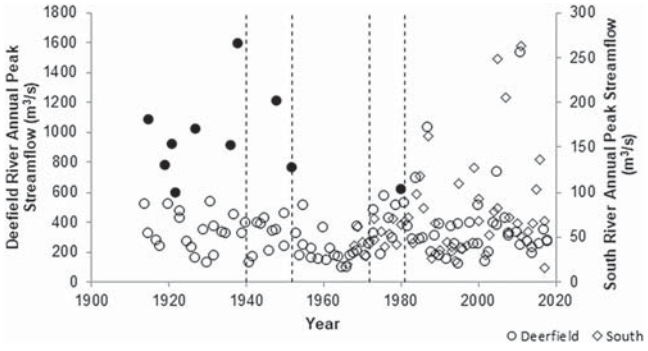

FIGURE 13. Annual peak streamflow from 1914 to 2018 obtained from USGS gage site 01168500, Deerfield River at Charlemont, MA, located within the Deerfield watershed, north of the South River (circles, left axis), and 1966–2018 from USGS gage site 01169900, South River near Conway, MA, located 4.2km upstream of the mouth (diamonds, right axis). Dashed vertical lines represent years 1940, 1952, 1972, and 1981 corresponding with aerial photographs and complete infilling of the Conway Electric Dam. Black circles are the 10 highest annual peak events from 1914 to 1981 on the Deerfield River.

Many of the dams in the watershed likely breached during the mid-nineteenth through mid-twentieth century, particularly related to large floods in 1869, 1904, 1936, and 1938 (Barten and Kantor, 2013). In particular, Barten and Kantor (2013) indicate that at least two mill dams breached and released impounded sediment around or after 1940, but before 1970 (Figures 2, 3), which likely resulted in a pulse of relatively high-Hg legacy sediment transported to the CED reservoir. The 1940–1952 interval also has the highest sediment yield (Figure 9; Table 1). This interval coincides with a decline in manufacturing and population in the area, occurring simultaneously with reforestation. As the area of agricultural land declined starting in the early twentieth century, New England was approximately 50% reforested by 1920 (Foster et al., 2008), and the pattern of decreased sediment yields generally follows this trend of increasing reforestation. In summary, we cannot quantify the relative importance of the various reasons for high sediment yield in the early twentieth century (including trap efficiency and flood events), and we suspect that dam breaches are likely the most important cause.

Pizzuto (2002) hypothesized that erosion of impounded sediment following dam removal begins with a rapid 'process driven' stage, followed by an 'event driven' stage dependent on floods. These stages have been observed at dam removal sites throughout the United States (e.g. Pearson et al., 2011; Sawaske and Freyberg, 2012; Collins et al., 2017; Major et al., 2017), and suggest an exponential decay of removal of reservoir sediment. Erosion of South River mill dam sediment following breaching likely followed a similar trend, and current erosion is now in the 'event driven' phase when sediment entrainment from exposed banks occurs primarily during rare high flow events. Previous studies observe that about 50% of the total volume is removed from non-cohesive (sand and gravel) reservoir deposits in less than two years of dam breaching, whereas it takes greater than two years (sometimes decades) for cohesive (clay and silt) deposits (Sawaske and Freyberg, 2012; Merritts et al., 2013; Major et al., 2017; Ritchie et al., 2018). Sediment removal from behind breached mill dams in the South River was likely rapid, as legacy sediment is primarily very fine sand (Table 3). We note however that most of the legacy sediment remains in the watershed as fill terraces. We document that this sediment was deposited on surfaces adjacent to the former millponds that were frequently inundated, and attribute it to the raised base level when the dams were in place (Johnson et al., 2019). Such sediment might not be included in the sediment budget of a dam removal, which tend to focus on the sediment stored in the reservoir (i.e. subaqueously), not adjacent landforms (cf. Pearson et al., 2011).

Contrary to our second hypothesis, our mixing model results are most consistent with glacial sources as the primary contributor of sediment in the latter half of the twentieth century (Table 2). In the Mid-Atlantic region, contemporary legacy sediment loads remain high and are a problem for suspended sediment and nutrient delivery to waterways, including the impaired Chesapeake Bay (e.g. Walter and Merritts, 2008; Donovan et al., 2015). However, the relative areal abundance of legacy sediment differs in New England due to its glacial history. Johnson et al. (2019) estimated that only 1.5% of the South River watershed area is comprised of legacy sediment. In the South River watershed, thick glacial deposits (primarily coarse stratified deposits) cover ~14% of the South River watershed. They suggest that the presence of legacy deposits is tied to the supply of upstream glacial material, and to natural sediment storage areas such as lakes or wetlands. The abundance of glacial sediment, deceleration in erosion rates soon after dam removals (e.g. Collins et al., 2017), and reactivation of glacial

Table 3. Mixing model inputs and calculated percent contributions of glacial and legacy sediment to the Conway Electric Dam (CED)

Mixing model	Mill Hg concentration (ppb/LOI)	Glacial Hg concentration (ppb/LOI)	CED Hg concentration (ppb/LOI)	Glacial contribution (%)	Legacy contribution (%)
Entire deposit (VC3 and VC5)	13.36	2.06	10.89	32 ± 10	68 ± 10
Pre-1953	13.36	2.06	11.33	26^{+35}_{-26}	74^{+26}_{-35}
Post-1953	13.36	2.06	8.84	63 ± 14	37 ± 14

mass failures (Yellen et al., 2014; Dethier et al., 2016) suggest these deposits are likely to remain as the dominant source as erosion of legacy exposures slows, and the channel recovers from eighteenth century to nineteenth century agricultural activity and damming. However, the large volume of legacy sediment that persists in the valley, accessed during high-flow events, is likely to remain a source of sediment from the watershed for decades to centuries (or longer).

Future analyses

Refined estimates from different source types could be accomplished through further analyses, either through the mixing model, or by developing a sediment budget (Walling and Collins, 2008; Gellis and Walling, 2011; Mabit et al., 2014). Using additional geochemical tracers, such as carbon (C) or nitrogen (N) isotopes related to agricultural activity (Mukundan et al., 2010; Belmont et al., 2014), or different instrumentation to identify additional trace metals could be used to develop a composite mixing model. This would categorize and distinguish different sediment sources more accurately, providing a more holistic representation of sediment contributions. In addition, incorporating sources such as hillslope soil would allow for the representation of contributions from different sources from the entire watershed to the CED reservoir, and would provide information on the upland source of legacy sediment. Additionally, temporal changes in factors such as Hg concentration of soils, land use, and erosion processes (sheetwash versus rill and gully erosion) would need to be considered, but are difficult to constrain.

Conclusions

We used sediments deposited in the CED reservoir from 1906 to 1981 to estimate sediment sources and yields from the South River watershed. Hg is an effective tracer to help distinguish the different source types in the South River watershed, and has been used at other sites (e.g. Skalak and Pizzuto, 2010). This study allowed for the investigation of erosion of legacy sediment over the past $>$ 100 years, bridging the gap between observations of legacy sediment erosion that begin decades after historic dam breaching and studies of recent dam removals. Erosion of high-Hg legacy deposits was more rapid during the early twentieth century (74^{+26}_{-35} %) likely as a result of dam breaching that released pulses of sediment from unvegetated reservoir deposits. This was followed by an increase in the relative contribution of erosion from glacial deposits, as represented by a significant decrease in Hg in the CED cores in the late twentieth century. Legacy sediment contributions decreased to 37 ± 14%, but still remain a substantial contribution through event-driven erosion. This trend is consistent with the pattern of high sediment yields in the early twentieth century, inferred from sedimentation rates in the CED reservoir.

Understanding fluvial readjustment to perturbations related to human land use compared to background erosion rates can inform the timescale of response to different generations of events. Overall, New England watersheds appear to display a rapid initial response to breaching of historic mill dams. Erosion of legacy sediment dominated the South River sediment load for the first half of the twentieth century, but appears to be a secondary source since then. This contrasts with studies on current legacy sediment erosion in the unglaciated Mid-Atlantic region, which could be inherently related to the availability of glacial-age deposits in New England. However, a large amount of legacy sediment persists in valley bottoms of the South River watershed, and can still be accessed during high flow events. This sediment will likely remain a source for centuries, as exponential decay equations from legacy sediment erosion of Mid-Atlantic reservoir sediments suggest these deposits can still contribute significant sediment for 50 to 100 years after breaching (Merritts et al., 2013). Restoration efforts would benefit from considering whether the long-term presence of legacy sediment in valley bottoms represents an important change to ecosystem services and functions, including flood storage, water quality, recreation, and habitat.

Acknowledgements—Thanks to Kate Johnson, Beth Ames, Megan McCusker Hill, Caitlin McManimon, and Maria Kopicki for their assistance in the laboratory and the field. The authors thank two anonymous reviewers and an associate editor for constructive suggestions, and two additional reviewers on an earlier draft. The Keck Geology Consortium, National Science Foundation grants 1062720, 1451586, and 1451562, and Geological Society of America grant 11229-16 all supported this work.

Conflict of Interest Statement

No conflicts of interest declared.

Data Availability Statement

The datasets used in the findings of this study are available from the corresponding author upon reasonable request.

References

Banks W, Gellis A, Noe G. 2010. Sources of fine-grained suspended sediment in Mill Stream Branch watershed, Corsica River Basin, a tributary to the Chesapeake Bay, Maryland [online] Available from: http://www.dnr.state.md.us/watersheds/tw/corsica/index.html.

Barten D, Kantor P. 2013. A River Runs Through Conway [Powerpoint slides]. Retrieved from http://www.friendsofthesouthriver.org/wpcontent/uploads/2013/03/RiverTalk_March2013_updated.pdf.

Belmont P, Willenbring JK, Schottler SP, Marquard J, Kumarasamy K, Hemmis JM. 2014. Toward generalizable sediment fingerprinting with tracers that are conservative and nonconservative over sediment routing timescales. *Journal of Soils and Sediments*, **14**: 1479–1492. https://doi.org/10.1007/s11368-014-0913-5

Bent GC. 2000. Suspended-sediment Characteristics in the Housatonic River Basin, Western Massachusetts and Parts of Eastern New York

and Northwestern Connecticut, 1994–96. US Department of the Interior, US Geological Survey: Reston, VA.

Blott SJ, Pye K. 2001. Gradistat: A grain size distribution and statistics package for the analysis of unconsolidated sediments. *Earth Surface Processes and Landforms*, **26**(11): 1237–1248. https://doi.org/10.1002/esp.261

Brena DC, Lin I, Watts CL, Newton RM, Merritt RB, Anderson MR. 2014. Soil mercury accumulation in O horizons from the Avery Brook watershed, West Whately, Massachusetts. *Geological Society of America Abstracts with Programs* **46**(2): 1–106.

Brune GM. 1953. Trap efficiency of reservoirs. *Eos, Transactions American Geophysical Union*, **34**(3): 407–418. https://doi.org/10.1029/TR034i003p00407

Collins AL, Walling DE, Leeks GJL. 1998. Use of composite fingerprints to determine the provenance of the contemporary suspended sediment load transported by rivers. *Earth Surface Processes and Landforms*, **23**(1): 31–52. https://doi.org/10.1002/(SICI)1, 096-9837(199801)23:1<31::AID-ESP816>3.0.CO;2-Z

Collins MJ, Snyder NP, Boardman G, Banks WSL, Andrews M, Baker ME, Conlon M, Gellis A, McClain S, Miller A, Wilcock P. 2017. Channel response to sediment release: insights from a paired analysis of dam removal. *Earth Surface Processes and Landforms*, **42**(11): 1636–1651. https://doi.org/10.1002/esp.4108

Dean WE. 1974. Determination of Carbonate and Organic Matter in Calcareous Sediments and Sedimentary Rocks by Loss on Ignition: Comparison With Other Methods. *SEPM Journal of Sedimentary Research*, **44**(1): 242–248. https://doi.org/10.1306/74D729D2-2B21-11D7-8648000102C1865D

Dearman TL, James LA. 2019. Patterns of legacy sediment deposits in a small South Carolina Piedmont catchment, USA. *Geomorphology*, **343**: 1–14. https://doi.org/10.1016/j.geomorph.2019.05.018

Dethier E, Magilligan FJ, Renshaw CE, Nislow KH. 2016. The role of chronic and episodic disturbances on channel–hillslope coupling: the persistence and legacy of extreme floods. *Earth Surface Processes and Landforms*, **41**(10): 1437–1447. https://doi.org/10.1002/esp.3958

Donovan M, Miller A, Baker M, Gellis A. 2015. Sediment contributions from floodplains and legacy sediments to Piedmont streams of Baltimore County, Maryland. *Geomorphology*, **235**: 88–105. https://doi.org/10.1016/j.geomorph.2015.01.025

Donovan M, Miller A, Baker M. 2016. Reassessing the role of milldams in Piedmont floodplain development and remobilization. *Geomorphology* **268**: 133–145. https://doi.org/10.1016/j.geomorph.2016.06.007

Doyle MW, Stanley EH, Harbor JM. 2002. Geomorphic analogies for assessing probable channel response to dam removal. *Journal of the American Water Resources Association*, **38**(6): 1567–1579. https://doi.org/10.1111/j.1752-1688.2002.tb04365.x

Doyle MW, Stanley EH, Harbor JM. 2003. Channel adjustments following two dam removals in Wisconsin. *Water Resources Research*, **39**(1). https://doi.org/10.1029/2002WR001714

Emerson BK. 1898. Geology of old Hampshire county, Massachusetts comprising Franklin, Hampshire, and Hampden counties. *Monographs of the United States Geologic Survey* Washington, DC: Government Printing Office, **29**: 782 p.1–782.

Field J. 2013. Fluvial Geomorphic Assesssment of the South River Watershed, Greenfield, MA: Unpublished report prepared for Franklin Region Council of Governments Greenfield MA on behalf of Field Geology Services, 108 p.

Foley MM, Bellmore JR, O'Connor JE, Duda JJ, East AE, Grant GE, Anderson CW, Bountry JA, Collins MJ, Connolly PJ, Craig LS. 2017. Dam removal: Listening in. *Water Resources Research*, 5229–5246. https://doi.org/10.1002/2017WR020457

Foster D, Motzkin G. 2009. 1830 Map of Land Cover and Cultural Features in Massachusetts: Harvard Forest Data Archive: HF122.

Foster DR, Donahue B, Kittredge D, Motzkin G, Hall B, Turner B, Chilton ES. 2008. New England's Forest Landscape: Ecological Legacies and Conservation Patterns Shaped by Agrarian History. *Agrarian Landscapes in Transition: Comparisons of Long-Term Ecological and Cultural Change*. 344.

Fox GA, Sheshukov A, Cruse R, Kolar RL, Guertault L, Gesch KR, Dutnell RC. 2016. Reservoir sedimentation and upstream sediment sources: Perspectives and future research needs on streambank and gully erosion. *Environmental Management*, **57**: 945–955. https://doi.org/10.1007/s00267-016-0671-9

Francis DR, Foster DR. 2001. Response of small New England ponds to historic land use. *Holocene*, **11**(3): 301–312. https://doi.org/10.1191/095968301666282469

Galster, JC, Pazzaglia, FJ & Germanoski, D. 2008. Measuring the impact of urbanization on channel widths using historic aerial photographs and modern surveys. *Journal of the American Water Resources Association*, **44**(4): 948–960. https://doi.org/10.1111/j.1752-1688.2008.00193.x

Gellis AC, Walling DE. 2011. Sediment source fingerprinting (Tracing) and sediment budgets as tools in targeting river and watershed restoration programs. *Geophysical Monograph Series*, 263–291. https://doi.org/10.1029/2010GM000960

Haddadchi, A, Ryder, DS, Evrard, O & Olley, J. 2013. Sediment fingerprinting in fluvial systems: Review of tracers, sediment sources and mixing models. *International Journal of Sediment Research*, **28**(4): 560–578. https://doi.org/10.1016/S1001-6279(14)60013-5

Horowitz AJ, Elrick KA. 1987. The relation of stream sediment surface area, grain size and composition to trace element chemistry. *Applied Geochemistry*, **2**(4): 437–451. https://doi.org/10.1016/0883-2927(87)90027-8

Howes FG. 1910. *A History of the Town of Ashfield Franklin County, Massachusetts from its Settlement in 1742 to 1910*: Ashfield, MA, Town of Ashfield 425 p.Town of Ashfield,

Jahns, R. H. 1947. Geological features of the Connecticut Valley, Massachusetts as related to recent floods. US Geological Survey Water Supply Paper. US Geological Survey: Reston, VA; 996, 1–158.

James LA. 2013. Legacy sediment: Definitions and processes of episodically produced anthropogenic sediment. *Anthropocene*, **2**: 16–26. https://doi.org/10.1016/j.ancene.2013.04.001

James LA. 2019. Impacts of pre- vs. postcolonial land use on floodplain sedimentation in temperate North America. *Geomorphology*, **331**: 59–77. https://doi.org/10.1016/j.geomorph.2018.09.025

Johnson KM, Snyder NP, Castle S, Hopkins AJ, Waltner M, Merritts DJ, Walter RC. 2019. Legacy sediment storage in New England river valleys: Anthropogenic processes in a postglacial landscape. *Geomorphology*, **327**: 417–437. https://doi.org/10.1016/j.geomorph.2018.11.017

Kamman NC, Engstrom DR. 2002. Historical and present fluxes of mercury to Vermont and New Hampshire lakes inferred from 210Pb dated sediment cores. *Atmospheric Environment*, **36**(10): 1599–1609. https://doi.org/10.1016/S1352-2310(02)00091-2

Kirchner G. 2011. 210Pb as a tool for establishing sediment chronologies: Examples of potentials and limitations of conventional dating models. *Journal of Environmental Radioactivity*, **102**(5): 490–494. https://doi.org/10.1016/j.jenvrad.2010.11.010

Koiter AJ, Owens PN, Petticrew EL, Lobb DA. 2013. The behavioural characteristics of sediment properties and their implications for sediment fingerprinting as an approach for identifying sediment sources in river basins. *Earth-Science Reviews*, **125**: 24–42. https://doi.org/10.1016/j.earscirev.2013.05.009

Kulp KP. 1983. Suspended-sediment characteristics of the Yantic River at Yantic. *Connecticut Water Resources Bulletin* **39**: 1–34.

Kulp KP. 1991. *Suspended-sediment characteristics of Muddy Brook at Woodstock, Connecticut: With a section on the water quality of Roseland Lake and its major tributaries, Muddy Brook and Mill Brook*. The Department of Environmental Protection: Hartford, CT.

Laceby JP, Evrard O, Smith HG, Blake WH, Olley JM, Minella JPG, Owens PN. 2017. The challenges and opportunities of addressing particle size effects in sediment source fingerprinting: A review. *Earth-Science Reviews*, **169**: 85–103. https://doi.org/10.1016/j.earscirev.2017.04.009

Mabit L, Benmansour M, Abril JM, Walling DE, Meusburger K, Iurian AR, Bernard C, Tarján S, Owens PN, Blake WH, Alewell C. 2014. Fallout ^{210}Pb as a soil and sediment tracer in catchment sediment budget investigations: A review. *Earth-Science Reviews*, **138**: 335–351. https://doi.org/10.1016/j.earscirev.2014.06.007

Macklin MG, Lewin J, Jones AF. 2014. Anthropogenic alluvium: An evidence-based meta-analysis for the UK Holocene. *Anthropocene*, **6**: 26–38. https://doi.org/10.1016/j.ancene.2014.03.003

Magilligan FJ, Nislow KH. 2005. Changes in hydrologic regime by dams. *Geomorphology* **71**: 61–78. https://doi.org/10.1016/j.geomorph.2004.08.017

Major JJ, East AE, O'Connor JE, Grant GE, Wilcox AC, Magirl CS, Collins MJ, Tullos DD. 2017. Geomorphic response to U.S. dam removals – a two-decade perspective. In *Gravel-Bed Rivers: Processes and Disasters*. John Wiley & Sons: Chichester; 832 p.

MassGIS. 2015. Surficial Geology (1:24,000). https://docs.digital.mass.gov/dataset/ massgis-data-usgs-124,000-surficial-geology.

McCusker MH, Daniels MD. 2008. The potential influence of small dams on basin sediment dynamics and coastal erosion in Connecticut. *Middle States Geographer* **41**: 82–90.

McCusker Hill M, Ouimet WB. 2015. Spatial analysis of gully erosion in southern New England. Geological Society of America Abstracts with Programs. Geological Society of America: Boulder, CO.

Merritts D, Walter R, Rahnis M, Cox S, Hartranft J, Scheid C, Potter N, Jenschke M, Reed A, Matuszewski D, Kratz L, Manion L, Shilling A, Datin K. 2013. The rise and fall of Mid-Atlantic streams: Millpond sedimentation, milldam breaching, channel incision, and stream bank erosion. *GSA Reviews in Engineering Geology*, **21**: 183–203. https://doi.org/10.1130/2013.4121(14)

Mukundan R, Radcliffe DE, Ritchie JC, Risse LM, McKinley RA. 2010. Sediment Fingerprinting to Determine the Source of Suspended Sediment in a Southern Piedmont Stream. *Journal of Environment Quality*, **39**(4): 1328–1337. https://doi.org/10.2134/jeq2009.0405

Mukundan R, Walling DE, Gellis AC, Slattery MC, Radcliffe DE. 2012. Sediment Source Fingerprinting: Transforming from a Research Tool to a Management Tool. *Journal of the American Water Resources Association (JAWRA)* **48**: 1241–1257. https://doi.org/10.1111/j.1752-1688.2012.00685.x

OCM Partners. 2020. 2012 FEMA Topographic Lidar: Hudson-Hoosic and Deerfield Watersheds, Massachusetts from 2010 to 06-15 to 2010-08-15. NOAA National Centers for Environmental Information, https://inport.nmfs.noaa.gov/inport/item/49774

Palazón L, Gaspar L, Latorre B, Blake WH, Navas A. 2015. Identifying sediment sources by applying a fingerprinting mixing model in a Pyrenean drainage catchment. *Journal of Soils and Sediments*, **15**: 2067–2085. https://doi.org/10.1007/s11368-015-1175-6

Pearson AJ, Pizzuto J. 2015. Bedload transport over run-of-river dams, Delaware, U.S.A. *Geomorphology*, **248**: 382–395. https://doi.org/10.1016/j.geomorph.2015.07.025

Pearson AJ, Snyder NP, Collins MJ. 2011. Rates and processes of channel response to dam removal with a sand-filled impoundment. *Water Resources Research*, **47**(8). https://doi.org/10.1029/2010WR009733

Pease CS (ed). 1917. *History of Conway (Massachusetts) 1,767-1917*. Springfield Printing and Binding Company: Springfield, MA 345 p.

Pennington W, Tutin TG, Cambray RS, Fisher EM. 1973. Observations on lake sediments using fallout137cs as a tracer. *Nature*, **242**: 324–326. https://doi.org/10.1038/242324a0

Perry E, Norton SA, Kamman NC, Lorey PM, Driscoll CT. 2005. Deconstruction of historic mercury accumulation in lake sediments, northeastern United States. *Ecotoxicology*, **14**: 85–99. https://doi.org/10.1007/s10646-004-6261-2

Pizzuto J. 2002. Effects of dam removal on river form and process. *BioScience* **52**: 683–691. https://doi.org/10.1641/00063568(2002)052[683:EODROR]2.0.CO;2

Pizzuto J, Skalak K, Pearson A, Benthem A. 2016. Active overbank deposition during the last century, South River. *Virginia. Geomorphology*, **257**: 164–178. https://doi.org/10.1016/j.geomorph.2016.01.006

Poff NL, Allan JD, Bain MB, Karr JR, Prestegaard KL, Richter BD, Sparks RE, Stromberg JC. 1997. A paradigm for river conservation and restoration. *BioScience* **47**: 769–784. https://doi.org/10.2307/1313099

Ritchie AC, Warrick JA, East AE, Magirl CS, Stevens AW, Bountry JA, Randle TJ, Curran CA, Hilldale RC, Duda JJ, Gelfenbaum GR, Miller IM, Pess GR, Foley MM, McCoy R, Ogston AS. 2018. Morphodynamic evolution following sediment release from the world's largest dam removal. *Scientific Reports*, **8**: 1–13. https://doi.org/10.1038/s41598-018-30817-8

Sawaske SR, Freyberg DL. 2012. A comparison of past small dam removals in highly sediment-impacted systems in the U.S. *Geomorphology*, **151**: 50–58. https://doi.org/10.1016/j.geomorph.2012.01.013

Skalak K, Pizzuto J. 2010. The distribution and residence time of suspended sediment stored within the channel margins of a gravel-bed bedrock river. *Earth Surface Processes and Landforms*, **35**(4): 435–446. https://doi.org/10.1002/esp.1926

Small IF, Rowan JS, Franks SW. 2002. Quantitative sediment fingerprinting using a Bayesian uncertainty estimation framework. IAHS-AISH Publiation: Wallingford.

Stone JR, DiGiacomo-Cohen ML. 2010. Surficial geological map of the Heath-Northfield-Southwick-Hampden 24-quadrangle area in the Connecticut Valley region, west-central Massachusetts: U.S. Geological Survey Open File Report 2006-1,260-G. US Geological Survey: Reston, VA.

Stout JC, Belmont P, Schottler SP, Willenbring JK. 2014. Identifying Sediment Sources and Sinks in the Root River, Southeastern Minnesota. *Annals of the Association of American Geographers*, **104**(1): 20–39. https://doi.org/10.1080/00045608.2013.843434

Thoms MC, Piégay H, Parsons M. 2018. What do you mean, 'resilient geomorphic systems'? *Geomorphology*, **305**: 8–19. https://doi.org/10.1016/j.geomorph.2017.09.003

Tomer MD, Locke MA. 2011. The challenge of documenting water quality benefits of conservation practices: A review of USDA-ARS's conservation effects assessment project watershed studies. *Water Science and Technology*, **64**(1): 300–310. https://doi.org/10.2166/wst.2011.555

Varekamp JC. 2006. The historic fur trade and climate change. *Eos*, **87** (52): 593–597. https://doi.org/10.1029/2006EO520002

Verstraeten G, Poesen J. 2000. Estimating trap efficiency of small reservoirs and ponds: methods and implications for the assessment of sediment yield. *Progress in Physical Geography*, **24**(2): 219–251. https://doi.org/10.1177/030913330002400204

Walling DE. 2005. Tracing suspended sediment sources in catchments and river systems. *Science of the Total Environment*, **344**(1): 159–184. https://doi.org/10.1016/j.scitotenv.2005.02.011

Walling DE, Collins AL. 2008. The catchment sediment budget as a management tool. *Environmental Science and Policy*, **11**(2): 136–143. https://doi.org/10.1016/j.envsci.2007.10.004

Walter RC, Merritts DJ. 2008. Natural streams and the legacy of water-powered mills. *Science*, **319**(5861): 299–304. https://doi.org/10.1126/science.1151716

Wohl E. 2015. Legacy effects on sediments in river corridors. *Earth-Science Reviews*, **147**: 30–53. https://doi.org/10.1016/j.earscirev.2015.05.001

Yellen B, Woodruff JD, Kratz LN, Mabee SB, Morrison J, Martini AM. 2014. Source, conveyance and fate of suspended sediments following Hurricane Irene. New England, USA. *Geomorphology*, **226**: 124–134. https://doi.org/10.1016/j.geomorph.2014.07.028